# Obtaining kinematic offsets for the kaon_lt experiment

December 21, 2025

G. Niculescu, I. Niculescu
James Madison University

## Contents

**1 Introduction** **2**

**2 Justification and approach** **3**
2.1 Original **heepcheck** . . . . . 3
2.2 **mmkc** approach . . . . . 4
2.2.1 Angular offsets . . . . . 5
2.2.2 Beam and spectrometer momentum offsets . . . . . 12
2.2.3 Implementation . . . . . 15

**3 Results** **19**
3.1 Missing mass alignment results . . . . . 19
3.2 Systematic uncertainty considerations . . . . . 23

**4 Conclusions** **27**

**References** **28**

# 1 Introduction

In the process of analyzing any physics data obtained with electromagnetic spectrometers, such as the HMS–SHMS pair in Hall C at Jefferson Lab, one needs to optimize the matrix elements (see, for example [1]) which provide the transfer function from the measured focal plane quantities to the target quantities. The latter can be used to compute the observables of interest. Most experiments also rely on extensive simulations which account for the known behavior of the spectrometer(s) and their associated detector packages.

However, the matrix fitting procedure mentioned above cannot account for the **kinematic offsets**[1] between the experimental data and its simulated "twin". There can be several reasons for these discrepancies: non-linearity in dipole/quadrupole current readouts, unevenness of the experimental hall floor, mis–alignment between the center of the target and the center of rotation of the spectrometer, etc.

The overdetermined exclusive electron–proton elastic scattering, $e + p \rightarrow e + p$, is used to study these offsets. In Hall C, a Fortran 77 program called **heepcheck** [2] is used for this purpose. The code evaluates the partial derivative of the invariant mass $W$ and of the missing energy and missing momentum with respect to spectrometer momentum and angle quantities. Hypothetical shifts in $W$, missing energy, etc. due to small offsets are also provided. The code is meant to be used interactively, with the human expected to figure out the best combination of offsets. **NOTE:** Even with the extra constraints provided by the elastic scattering, the system is under–determined so **heepcheck** cannot provide a unique set of offsets, thus the need for human input.

In this note we describe an alternate way of determining kinematic offsets which, while inspired by the original **heepcheck** work, differs from it in substantial ways. Section 2 provides the motivation and approach adopted here, while section 3 shows the results of this study. Our conclusions and further recommendations are in section 4.

[1] Also known as zero-th order matrix elements.

# 2 Justification and approach

## 2.1 Original heepcheck

The original **heepcheck** code was developed in an era when the maximum beam energy at JLab was 4 GeV. At this energies the elastic scattering cross–section is substantial, resulting in abundant statistics for **heepcheck** studies. With the upgrade of the JLab beam energy to the present day (end of 2025) 10.5 GeV (in Hall C), most experiments aim for higher $Q^2$ kinematics. At high $Q^2$ the elastic cross–section is significantly smaller. Ideally, an experiment should have **heepcheck** data (with good statistics!) for each electron arm momentum–angle combination. Due to time constraints it becomes impractical to acquire this type of data for all kinematics. In particular, the kaon_lt experiment took only a limited set of elastic electron–proton data.

In addition to the practical constraints listed above, several issues associated with the original **heepcheck** code were identified:

- the partial derivatives that heepcheck.f calculates assumes that the elastically scattered electron and proton are ALWAYS in the center of their respective spectrometer. So $\delta_e = 0$, $\delta_p = 0$ and the in–plane and out–of–plane angles (with respect to the central angle) are also at zero.

- while there are constraints between the electron and proton momenta and angle, the elastic kinematics extend beyond the very center of each spectrometer. The formulas used to calculate the partial derivatives do not take this into account.

- in particular, the out–of–plane angle is not included. Reference [2] erroneously assumes that the electron scattering angle (i.e. the angle between the incoming beam and the scattered electron) only has a horizontal component.

- the code assumes that beam energy is always constant and that is has no $x$ and $y$ components. In reality, the beam can sport a small angle (thus $x$ and $y$ components) and it has, especially at the larger energies, a noticeable spread [3].

- besides being written in Fortran (which raises maintainability issues), the code does not provide any guidance on selecting the best set of offsets.

- while the code itself allows for offsets in beam energy, reference [2] argues against this, on the grounds that the potential shifts are much smaller than the resolution in $W$, missing momentum, etc. While that might have been true in the JLab 4 GeV era, at 12 GeV the beam has, according to Table I from Reference [3] a 2-3 MeV spread. Figure 1 shows the typical arc–corrected beam energy for one of the 10.6 GeV kaon_lt runs.

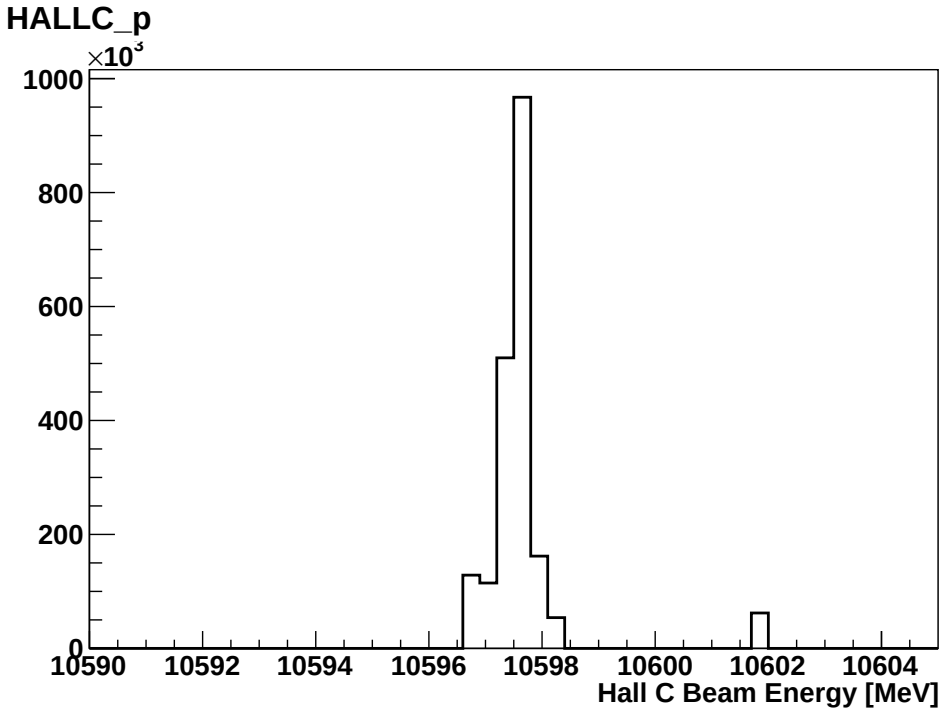


Figure 1: Arc–corrected beam energy (in MeV) from the hcana ROOT file for run 4865.

## 2.2 mmkc approach

In order to obtain a credible and consistent set of kinematic offsets we developed an alternative procedure, conventionally named **mmkc** - missing mass Kaon check. While our algorithm takes advantage of the specifics of the kaon_lt experiment, it can be easily generalized to other two–arm spectrometer data. Furthermore, we provide a straightforward way of evaluating the systematic uncertainty associated with the use of these offsets.

Nine quantities that potentially have offsets were identified. All of these quantities contribute in calculating the missing mass in the $e + p \rightarrow e' + K^+ + Y$ reaction. In no particular order, these are: the spectrometer central momentum ($p_0$) and the in–plane and out–of–plane quantities ($yptar$ and $xptar$) for HMS and SHMS and the momentum components of the beam ($p_x$, $p_y$, $p_z$, with the $z$ direction being the nominal beam direction, as usual). For completeness and in order to facilitate comparisons with similar offset–finding efforts carried out in parallel with this work, these offsets were implemented as follows:

- central momentum correction was cast as multiplicative percentages:
  $p_{0\,new} = p_0 \cdot (1 + central_{offset}/100)$

- $p_{z\,new} = p_z \cdot (1 + ebeam_{offset})$
- $p_x$ and $p_y$ were simple additive corrections: $p_{x\,new} = p_x + p_{x\,offset}$
- the angles were cast as simple additive corrections to their base quantities.
- the **HallC_p**, the arc–based measurement of the beam energy, is used as the basis for $p_z$. This in contrast with the original **heepcheck**, which used a single, fixed beam energy.
- the original **heepcheck** argued for a common set of offsets that will account for most/all of the shifts in $W$ (as well as the other elastic constraints). This would be true if said offsets are purely instrumental in nature (for example if the magnet reading would be off by the same, possibly scaled, amount for all settings). However, experience in Hall C operations showed that some effects are highly kinematic dependent (spectrometer mis–pointing, uneven floor, saturation effects). Therefore, instead of attempting to find a common set of offsets for all kinematic settings, we developed sets of offsets for each.
- **NOTE:** Please note that given the implementation above, these offsets are tightly linked with the central values for the spectrometer momentum and angle and all potential comparisons with similar efforts should take this into account[2]

### 2.2.1 Angular offsets

The ultimate goal of this offset–finding exercise is to see all the prominent peaks in the missing mass spectrum align with their expected values (see 2.2.2). Before attempting to find the optimum set of offsets in a nine–dimension space with only three constraints, we first observe that the in–plane and out–of–plane quantities *xptar* ($-ph$ in **hcana** notation) and *yptar* ($-th$ *ditto*) depend only on their respective offsets. Furthermore, in the typical analysis, one does not place stringent/limiting cuts on these variables. Figures 2 to 5 show distributions of these four observables, as obtained from **simc**, for several 10.6 GeV kinematics. As it can be seen from these graphs, the edges of each of the distributions (and especially the endpoints) do not depend on the kinematics.

[2]In this work we used the github version of the kaon_lt kinematics, as developed by R. Trotta.

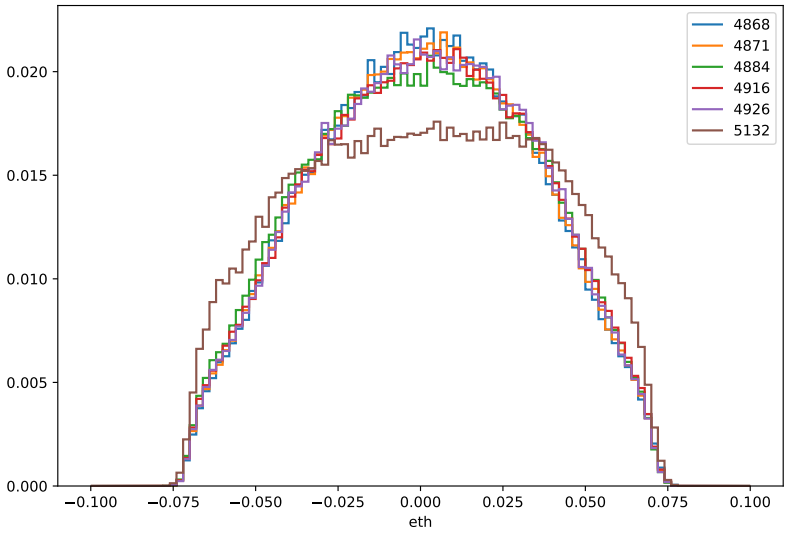


Figure 2: Simulated HMS *xptar* distribution for several representative 10.6 GeV kinematics.

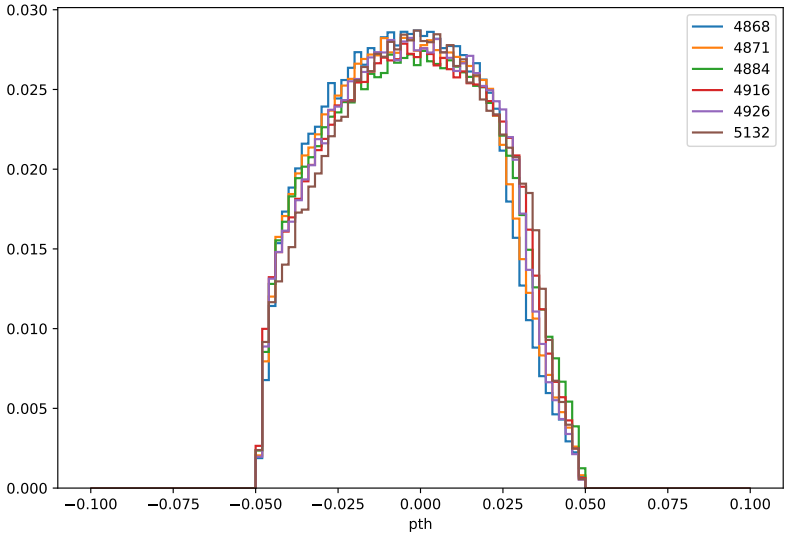


Figure 3: Simulated HMS *yptar* distribution for several representative 10.6 GeV kinematics.

This is in agreement with the basic understanding of a small angle electromagnetic spec-

trometer that uses an entrance collimator. The shadow of the collimator, combined with the weak correlation between the electron and the hadron arm (as the reactions of interest are 3–body final states), imply that the edges of these distributions depend mostly on geometry and magnetic fields rather than the physics reaction(s) studied.

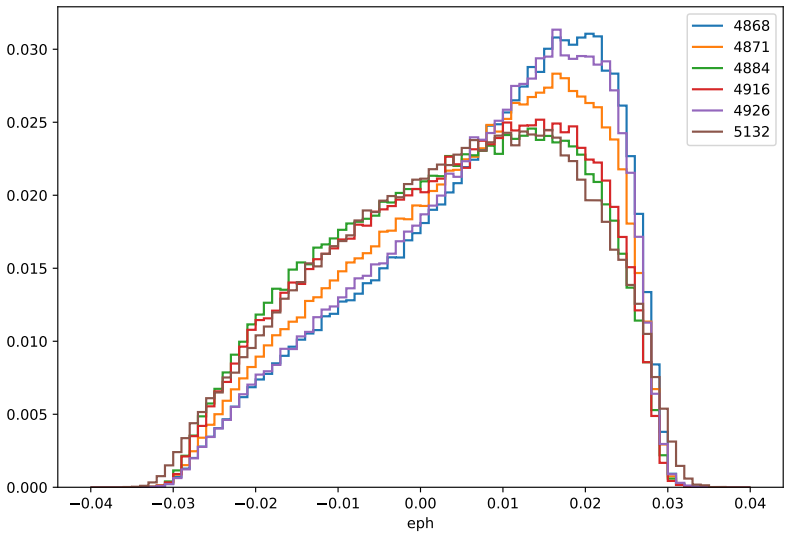


Figure 4: Simulated SHMS *xptar* distribution for several representative 10.6 GeV kinematics.

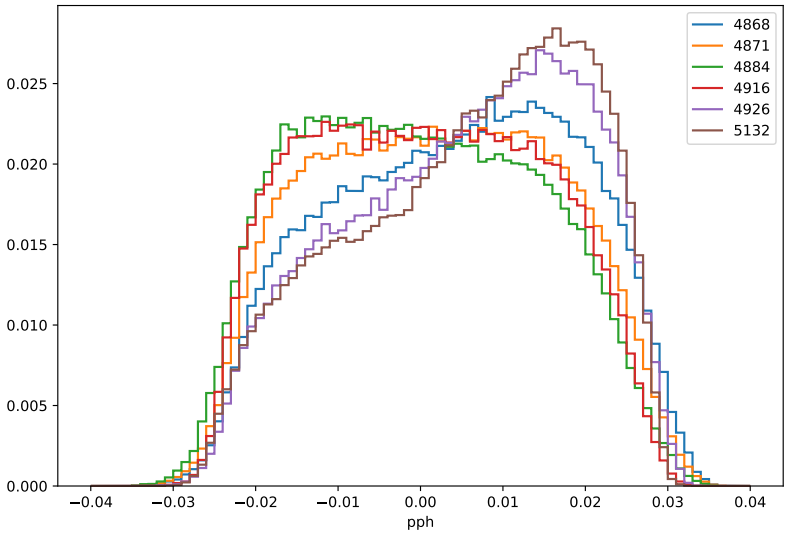


Figure 5: Simulated SHMS *yptar* distribution for several representative 10.6 GeV kinematics.

In this work, the in–plane and out–of–plane angle offsets were treated independently. For each angle a *low* and a *high* region were defined, as seen in Figure 6.

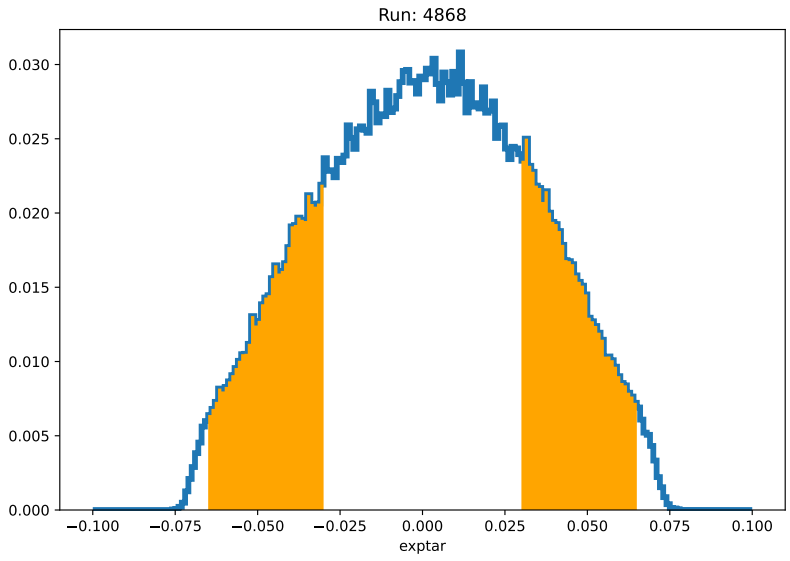


Figure 6: Simulated HMS *xptar* distribution for one of the 10.6 GeV kinematics. The full distribution is shown in blue, while the edges retained for the offset–finding algorithm described in the narrative are shown in solid orange.

The integral of these distributions was obtained from both the data and the simulation: $I_{ld} = I^{data}_{low}$, $I_{hd} = I^{data}_{high}$, $I_{lmc} = I^{simc}_{low}$, $I_{hmc} = I^{simc}_{high}$. The data and Monte Carlo distributions were cross–normalized by multiplying the **simc** histograms with the ratio:

$$C = \frac{I_{ld} + I_{hd}}{I_{lmc} + I_{hmc}} \tag{1}$$

To find the best possible offset, the data distribution was shifted systematically (in the ±6 mr range), the data integrals and the constant $C$ were re–evaluated each time, and following cost function was minimized:

$$cost\_function = \sum_{i=(l,h)} (I_{id} - C \cdot I_{imc})^2 \tag{2}$$

Figure 7 attempts to illustrate this algorithm: the **simc** *xptar* distribution is shown in orange, while the histograms in red show the data distribution with various offsets applied. Only the *low* edge of the distribution is shown. This procedure worked successfully for all four angles and all 10.6 GeV settings. Sample plots are shown in Figures 8 and 9. A small distortion is observed in the SHMS angles, with the data and the simulated distributions sporting slightly different width, which cannot be reconciled with offsets alone!

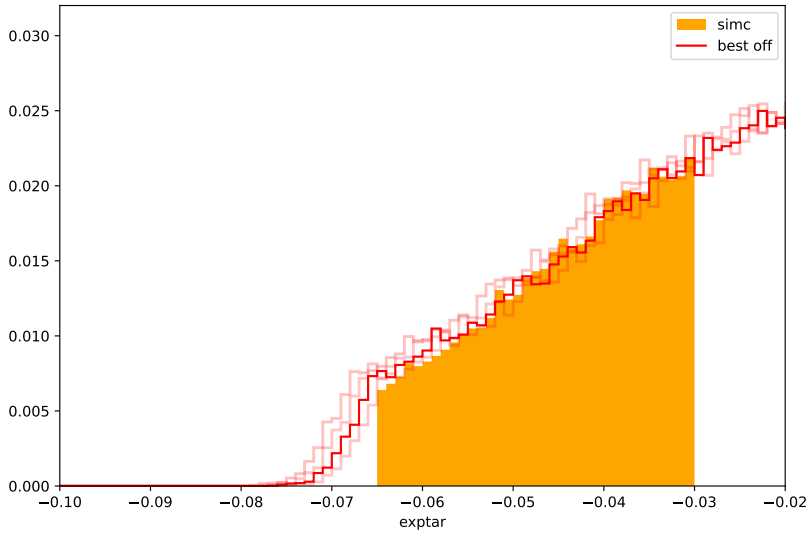


Figure 7: Illustration of the angle offset finding using edge matching. The **simc** distribution is shown as solid orange, while the data distributions with a few different offsets are shown in various shades of red.

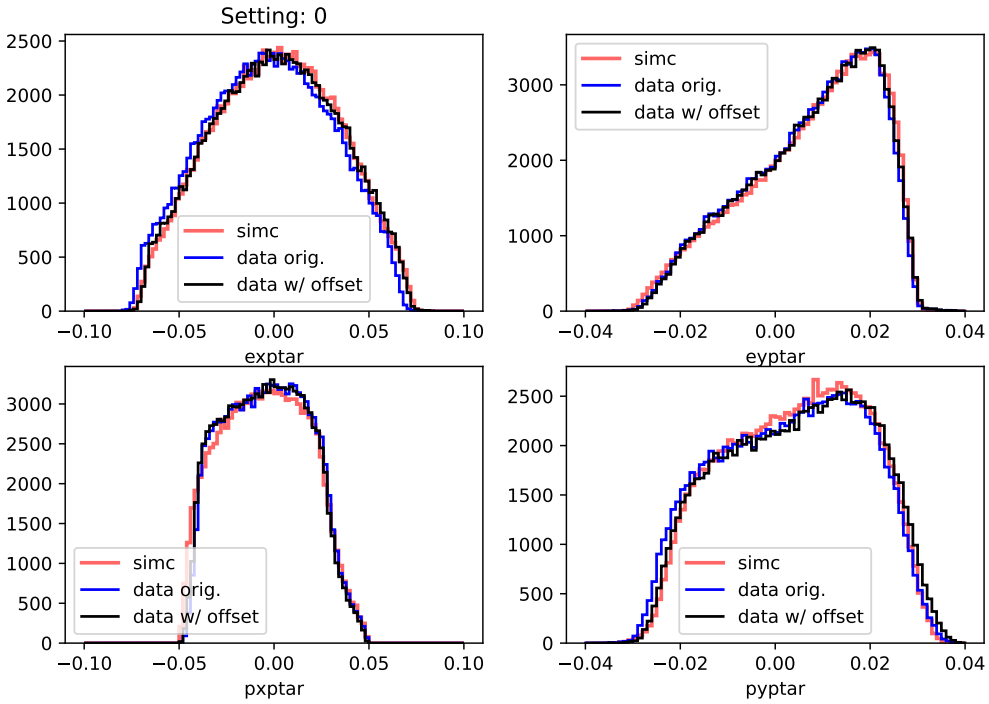


Figure 8: Angular offsets for kinematic setting 0. Before, after, and simc distributions are shown.

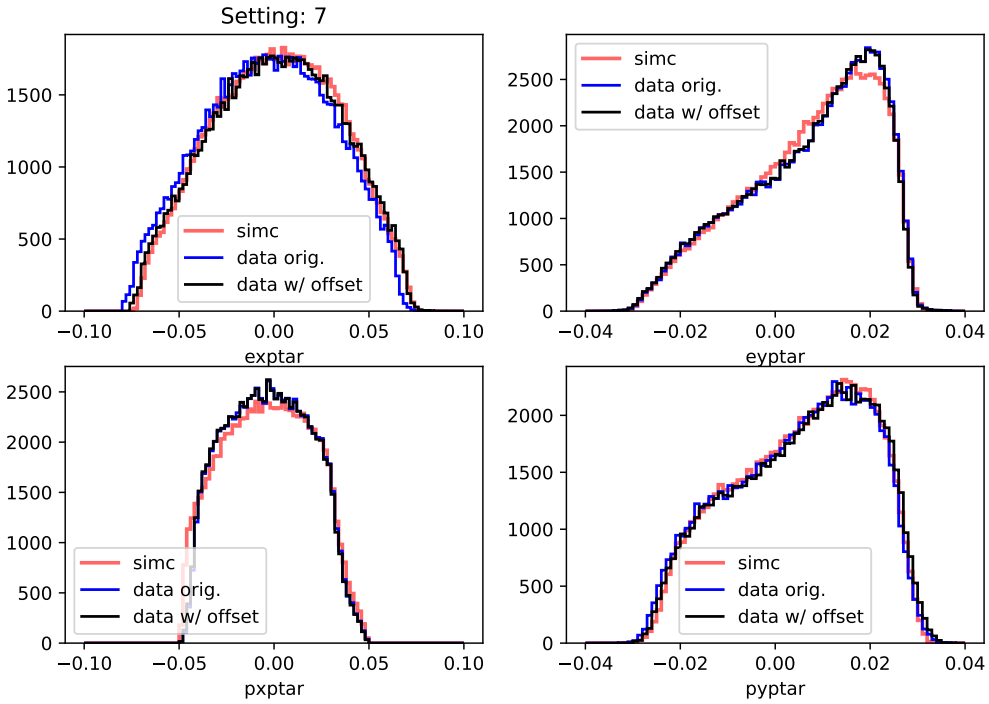


Figure 9: Angular offsets for kinematic setting 7. Before, after, and simc distributions are shown.

### 2.2.2 Beam and spectrometer momentum offsets

The in–plane and out–of–plane offsets determined as explained above were used as the starting point for the offset–finding procedure, described below. In principle one could have opted to keep *xptar* and *yptar* fixed. For more flexibility, in this work a small variation (below 0.03 mr for each angle) was allowed.

As the **kaon_lt** acquired electron–kaon coincidence data, the missing mass spectrum has prominent peaks for the $\Lambda$ and $\Sigma^0$ hyperons, as well as an additional peak corresponding to the positive pions that leak through the kaon identification cuts. The positions of the $\Lambda$ and $\Sigma^0$ peaks are known (from **simc** Monte Carlo), as is the position of the pion missing mass peak. **NOTE:** for the latter observable one needs to use the actual mass of the $\pi^+$ meson when calculating the missing mass, and not the (default for this experiment) $K^+$ mass. Figures 10 and 11 show the missing mass $e + p \rightarrow e' + \pi^+ + X$ as a function of the hadron arm $\delta$ using the $K^+$ mass and, respectively, using the $\pi^+$ mass. The missing mass no longer depends on the hadron momentum (which it should not!) and it is a lot closer to

the expected neutron mass $(0.939\ GeV/c^2)$[3]

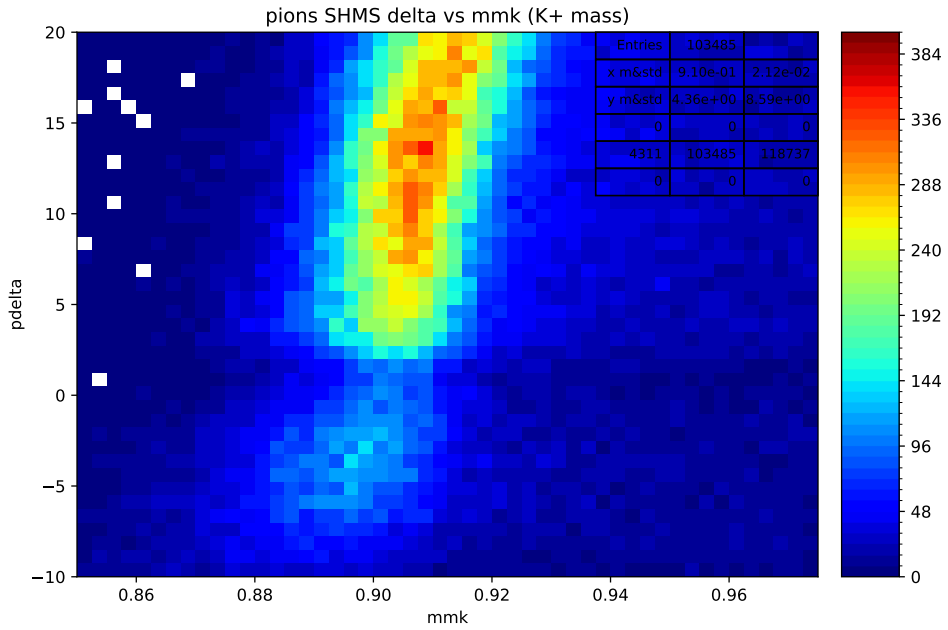


Figure 10: $e + p \rightarrow e' + \pi^+ + X$ as a function of the SHMS $\delta$. Missing mass was reconstructed using the "default" $K^+$ mass.

The three baryon masses mentioned above ($\Lambda$, $\Sigma^0$, and $n$) are the foundation on which the **mmkc** *cost function* is constructed. For this work, we calculate a $\chi^2$–like function:

$$cost\ function = \sum_{i=1}^{3} (mm_{data} - mm_{simc})_i^2 \tag{3}$$

where $mm_{data}$ is the missing mass distribution as obtained from the experimental data, $mm_{simc}$ is the expected value for the missing mass (as predicted by **simc** for the current kinematic setting), the index $i$ denotes each of the three baryon regions of interest (ROI).

[3]In reality the peak should be at a slightly larger value than the neutron mass, as expected because of radiative corrections and as predicted by **simc**.

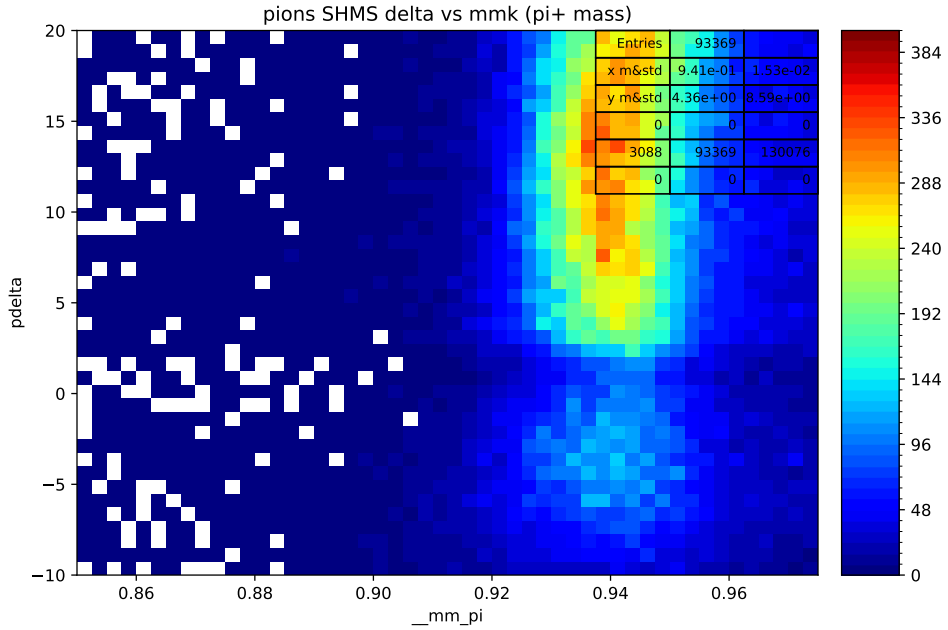


Figure 11: $e+p \rightarrow e'+\pi^{+}+X$ as a function of the SHMS $\delta$. Missing mass was reconstructed using the correct $\pi^{+}$ mass.

The goal is to minimize this cost function with respect to the possible spectrometer and beam offsets. As there are only three constraints and nine degrees of freedom, finding the optimum set of offsets is an ill–defined problem (just like the original **heepcheck** work). For this study we used a *metaheuristic* approach, namely a *genetic algorithm*:

**Step 0**

- Randomly generate a large set of offsets (in this study we used 1000 for each kinematic setting), uniformly within a "reasonable" range for each variable: $\pm 0.3$ for the HMS/SHMS momentum, 0.003 for the beam components[4], and 0.03 mr for all angle offsets.

- For each set of offsets all kinematic variables were recalculated based on the original ROOT data, all relevant cuts were applied, and the missing mass for both the kaon and the positive pion were obtained.

[4]all these values only make sense within the offset formulas given earlier

- For each of the three ROIs, the position of the peak was obtained using a simple Gaussian fit. The position of these peaks were used in Eq. 3 to calculate the cost function.

- To avoid potential local minima, the best $n$ sets of offsets were selected for further study. For the work reported here $n = 10$.

**Step 1**

- Each of the $n$ offsets identified in **Step 0**, becomes the "seed" (parent?) for the next generation of offsets. The new offsets were generated symmetrically around their "parent" value, with a smaller range (by a factor of two) than the previous generation.

- The same recalculation of kinematic variables, followed by fitting the missing mass peaks was carried out, and the new sets of $\chi^2$s were obtained.

- The best $n$ offsets were identified and earmarked for further studies.

**Step 2**

- The procedure above was followed one more time. For the results below, only the most promising of these third generation offsets were used.

### 2.2.3 Implementation

Figures 12 and 13 illustrate the **mmkc** offset–finding algorithm described above. This algorithm was incorporated in the larger **jmu_klt** software package [5], as an intermediate step between the initial data reduction/DST–writing and the yield extraction.

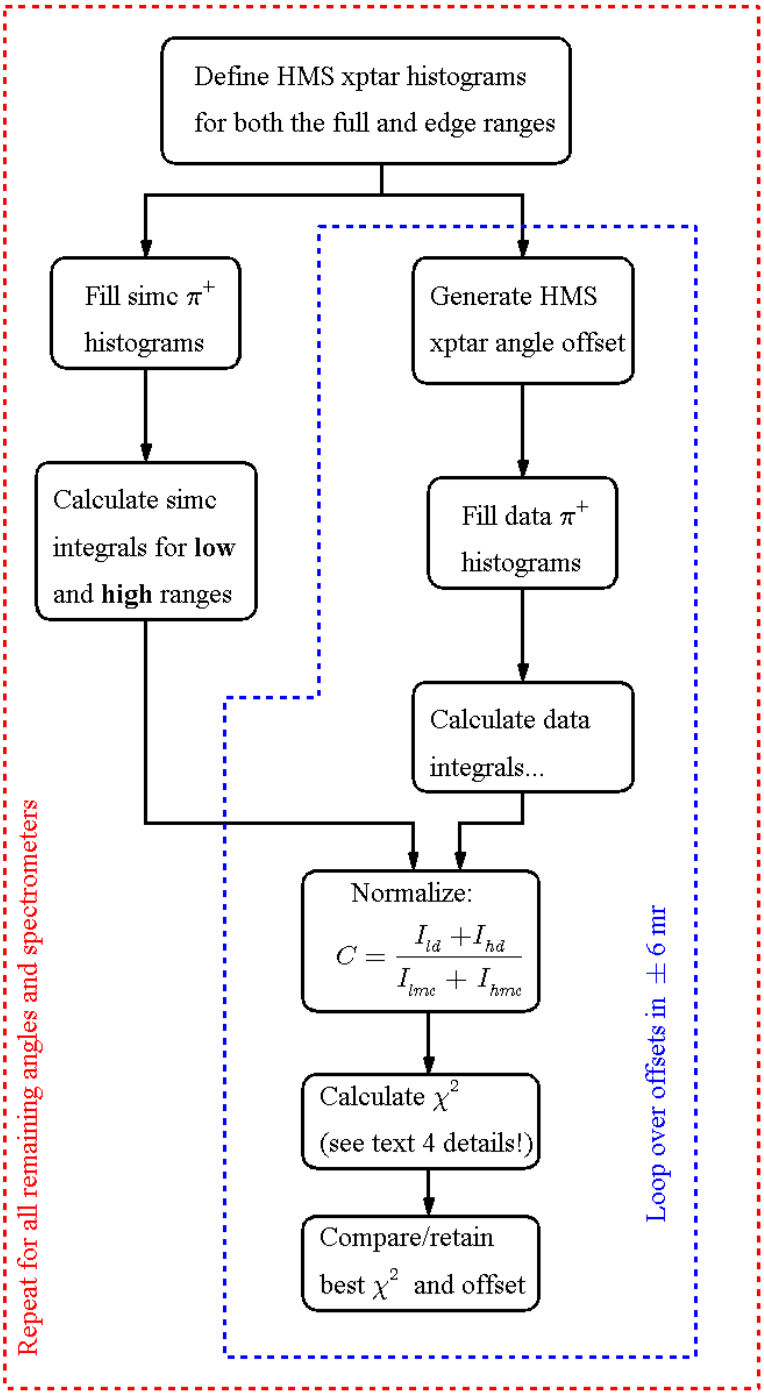


Figure 12: Chart describing angular offset–finding method. This procedure is carried out, separately, for each kinematic setting.

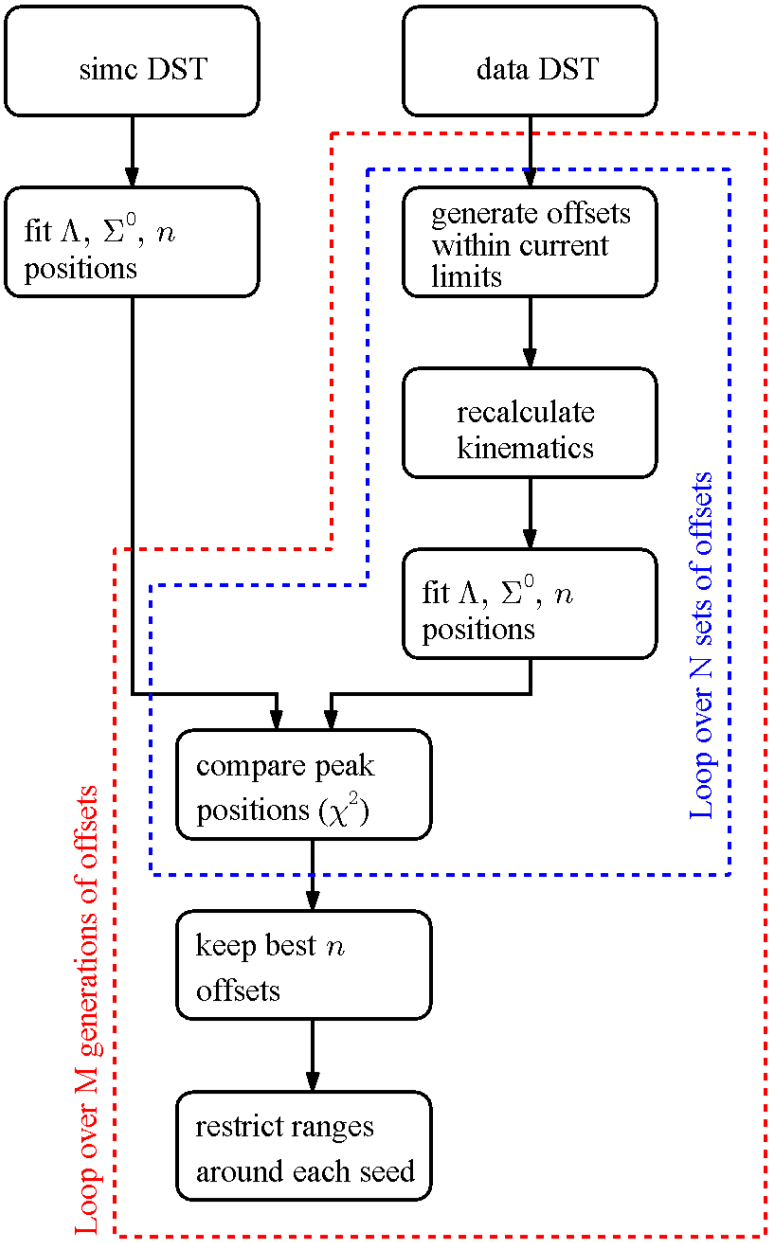


Figure 13: Chart showing the algorithm for beam and spectrometer momentum offsets. This procedure is carried out, separately, for each kinematic setting.

The code takes full advantage of the **lmfit** [6] module for carrying out the (many!) fitting procedures needed. Furthermore, upgrading our code to python 3.14 enabled running several

(at least two!) instances in parallel, without the added overhead of multi–threading, as 3.14 is the first python version without a **GIL** (Global Interpreter Lock).

# 3 Results

## 3.1 Missing mass alignment results

The edge–finding and peak position optimization algorithm described in Section 2 was carried out for all 10.6 GeV settings. Figures 14 to 17 show the kaon and positive pion missing mass distributions before and after implementing the best set of offsets for one of the kinematic settings.

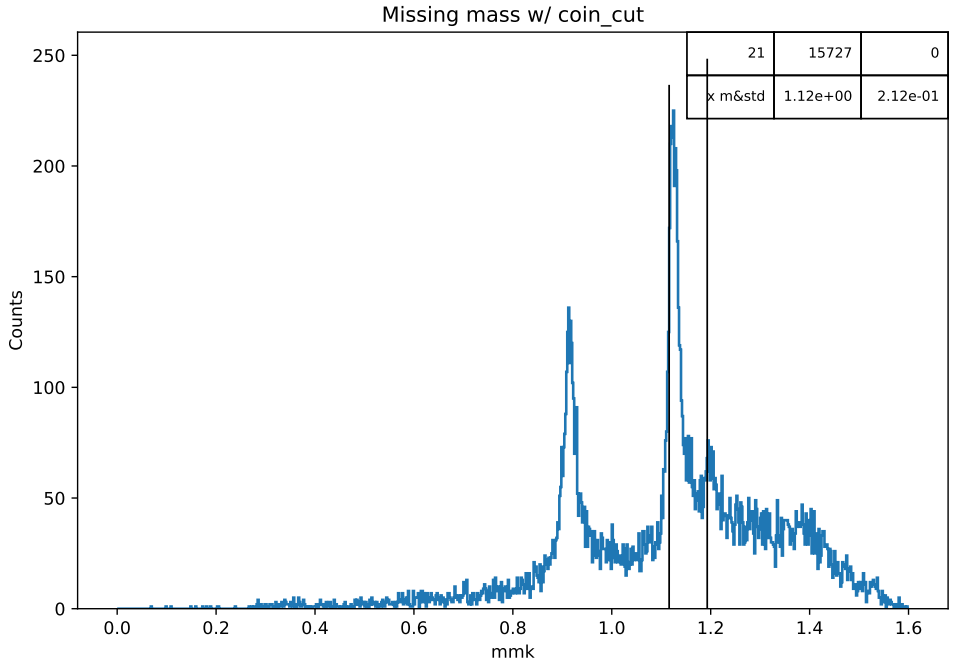


Figure 14: $e + p \rightarrow e' + K^+ + Y$ missing mass without offsets.

For each of these figures the vertical lines correspond to the expected missing mass peaks for $\Lambda$, $\Sigma^0$, and, respectively, $n$ as obtained from **simc**. For completeness, Figure 18 shows the fit of the simulated missing mass peak with both a Gaussian as mentioned above as well as using a skewed Voigtian function [4].

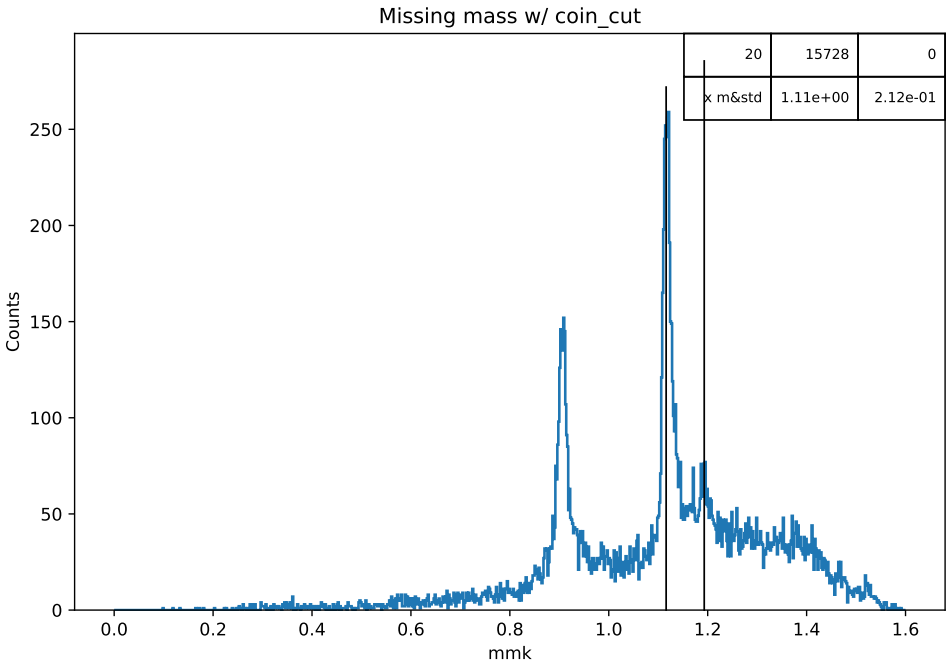


Figure 15: $e + p \rightarrow e' + K^+ + Y$ missing mass after applying offsets.

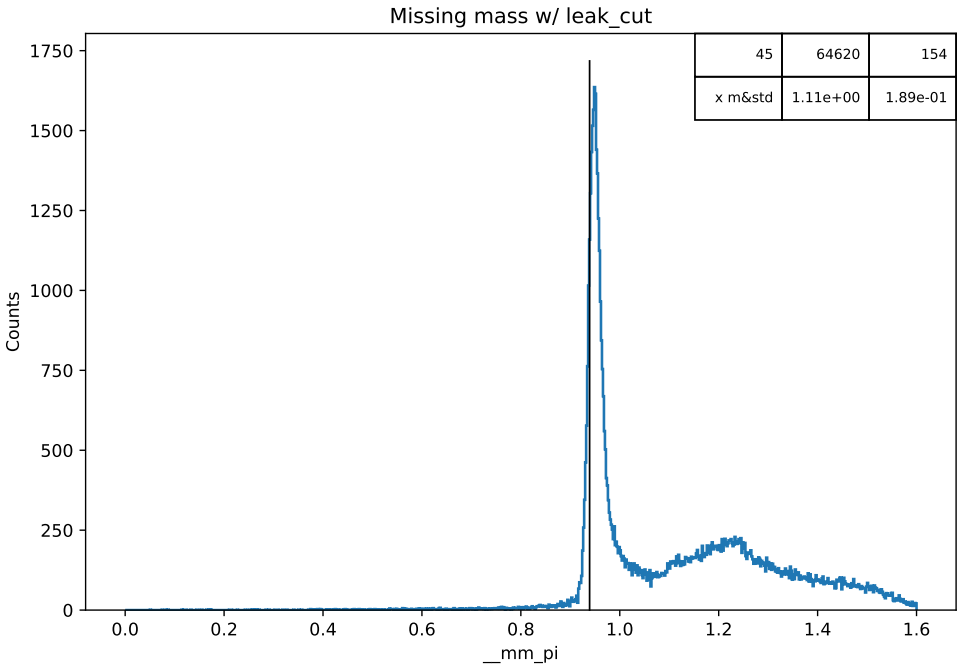


Figure 16: $e + p \rightarrow e' + \pi^+ + X$ missing mass without offsets.

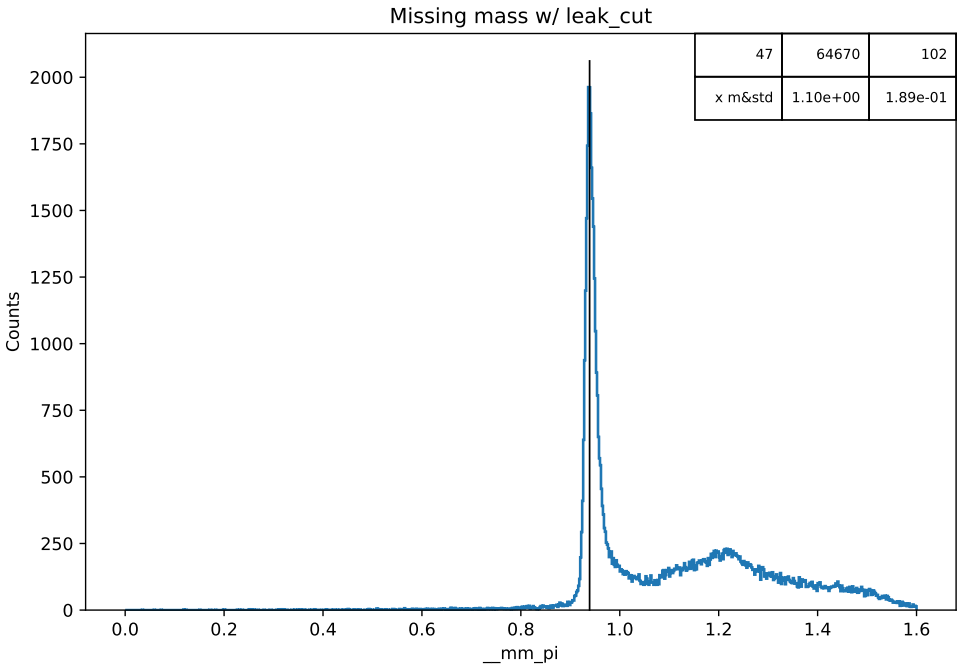


Figure 17: $e + p \rightarrow e' + \pi^+ + X$ missing mass after applying offsets.

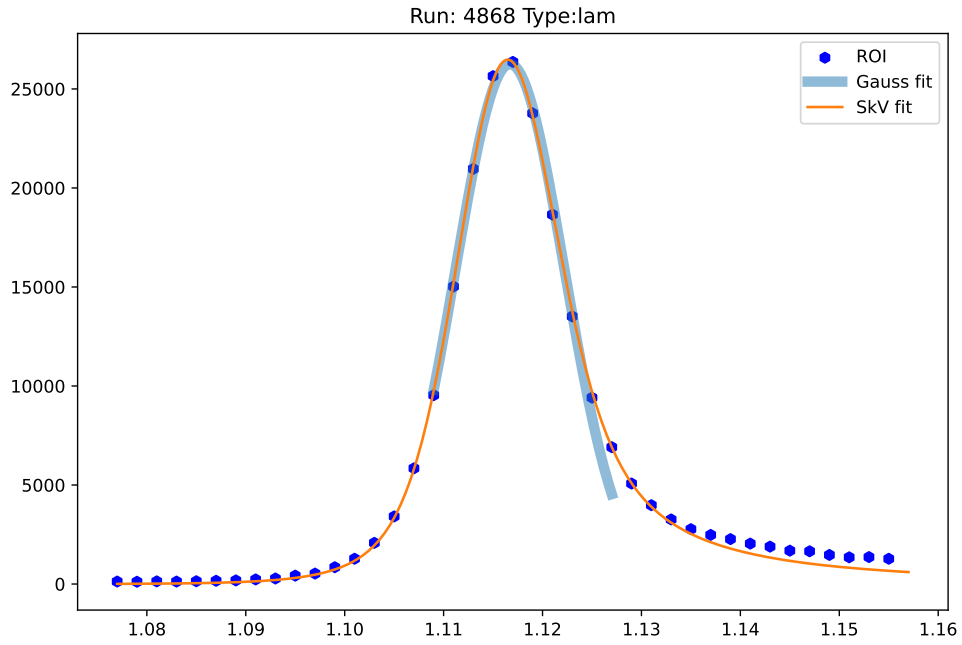


Figure 18: Fitting the simulated $e + p \rightarrow e' + K^+ + \Lambda$ missing mass peak with a Gaussian (thick blue line) and a skewed Voigt (orange line) functions.

## 3.2 Systematic uncertainty considerations

The missing mass spectra and the angular distributions obtained using the offsets estimated as described in this study look encouraging, as they align well with their "digital twins" obtained via **simc** simulations. However, the offset–finding problem is under–determined as there are not enough constraints to enable us to choose "the best" set of offsets. Indeed, the genetic algorithm we developed succeeds in producing several sets of offsets having a similar *cost function* (proxy for $\chi^2$). A typical cost function distribution is show in Figure 19: the full range of cost functions retained for further study[5] across all three generations simulated is shown in black while the subset of the "best" third generation sets of offsets is shown in red.

[5]For generations 0 and 1 only the best 10 sets were retained.

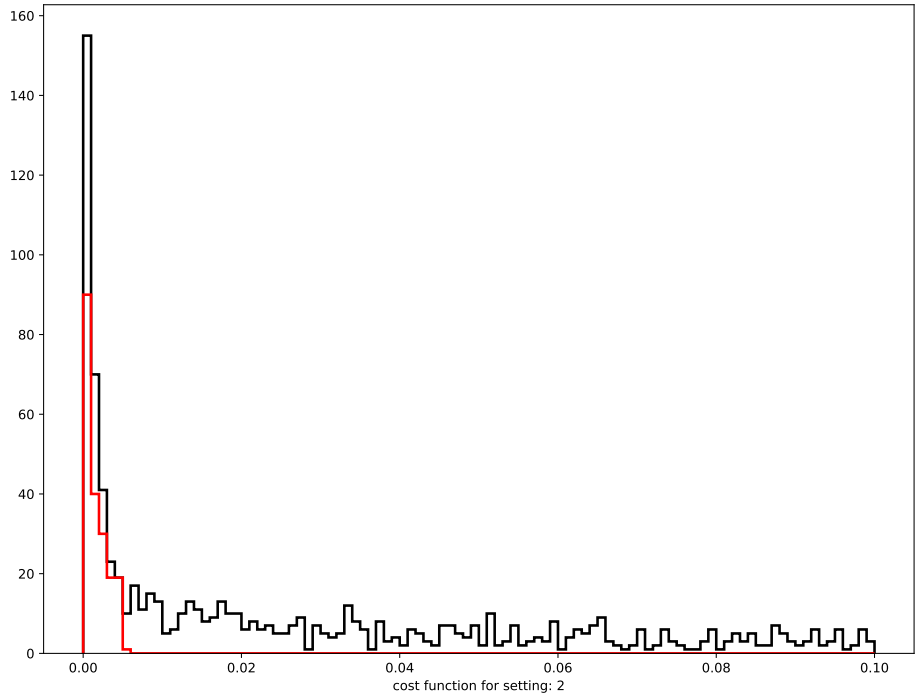


Figure 19: Distribution of the *cost function* ($\chi^2$) for kinematic setting 2. The distribution for the cost functions retained across all three generations is shown in black while the distribution of the generation 2 subset of "best" cost functions is shown in red.

Figure 20 shows the range of all nine offsets for the same kinematic setting as in Figure 19. Only the "best" third generation offsets are shown. As expected, the range of these offsets is small: MeV–range for the momentum–type offsets and (a fraction of a) *mr* for the angle variables. Also note the mirror–like shape of some of the distributions, for example *ebeam_offx* and *ebeam_offy*: as we have more degrees of freedom than constraints, we can obtain viable/plausible offsets with a positive offset in *ebeam_offx* and a negative one in *ebeam_offy*, or the other way around. A similar logic would apply to HMS/SHMS out–of–plane offsets: as one spectrometer gets a positive out–of–plane angle the other will get a negative offset, and the physics will still be consistent[6].

[6]Luckily, the edge–matching trick helped solve this problem.

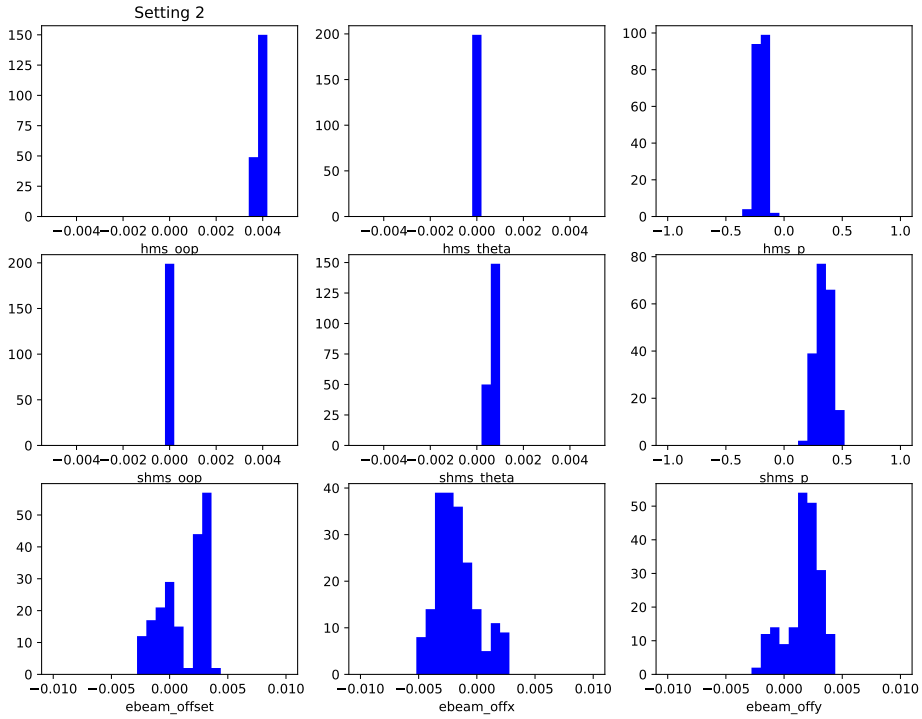


Figure 20: Third generation offset distributions for kinematic setting 2. Only the "best" sets (red distribution in Figure 19 are shown.

Studying the range, correlation, and kinematic (central momentum and angle) dependence (or lack thereof) of these offsets is an interesting topic in itself and it would (especially if extended to a few more experiments) be a worthwhile[7] master–level thesis (or even an undergraduate Honor's thesis). This is beyond the scope of this work. A more pressing/pragmatic question is gauging the effect of using these offsets in the subsequent analysis.

To study the systematic uncertainties introduced by the kinematic offsets in the final result, we used the set of third generation "best" (200 or so) offsets. For each of these sets of offsets all kinematic quantities were recalculated (starting with the original ROOT DST files). The $\pi^+$ missing mass spectrum was used to obtain the neutron peak yield (in the 0.85–1.05 GeV range)[8]. Figure 21 shows the "normalized yield" for the typical setting (kinematic 2). Please note that the "normalized yield" quantity uses the usual definition employed in Machine Learning/Artificial Intelligence algorithms, i.e. subtracting the mean

[7] In the author's opinion.

[8] as they are substantially more abundant and have less background compared to hyperons

($Y_m$) from each yield ($Y_i$) and dividing by the standard deviation ($\sigma$):

$$norm.\, Y_i = \frac{Y_i - Y_m}{\sigma} \tag{4}$$

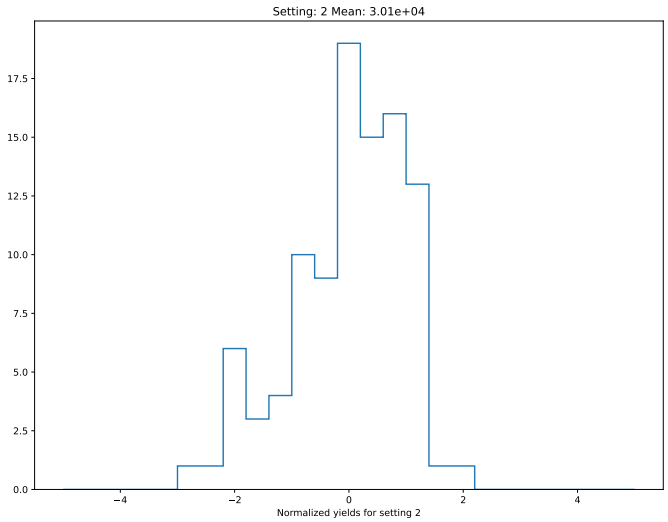


Figure 21: Normalized yield distribution for kinematic setting 2.

The standard deviation of the yield was used as a measure of the systematic uncertainty due to the kinematic offsets. Even though this estimate is based on the $\pi^+$ missing mass peak, we cannot envision any mechanism that will make this effect different between pions and kaons, therefore this is the uncertainty that will be assigned to the hyperon yields. For all 10.6 GeV kinematics studied, this uncertainty was quite small, at the level of 0.05%.

# 4 Conclusions

At ∼10 GeV beam energies (and, most of the time, large $Q^2$ values) using coincidence electron–proton elastic scattering data to infer the spectrometer momentum and angle offsets (zero–th order matrix elements) becomes impractical (low statistics, prohibitively large DAQ times). Furthermore, **heepcheck.f**, the code traditionally used in Hall C to estimate these offsets, has substantial theoretical (central kinematics in both spectrometers, no out–of–plane angles for scattering angle calculations, etc.) and practical (the dwindling number of active fortran programmers, lack of automation, etc.) limitations.

We introduce an alternative, experimental data–centered approach, for offset–finding. While the algorithm was developed in the context of the **kaon_lt** experiment, its ideas can easily be generalized for other data sets. In essence, the code is physics–guided search in a nine–dimensional space that leverages both the understanding of small–aperture magnetic spectrometers (for angle offset finding) and the position of sharp features in the data (peaks in missing mass spectra).

This was implemented as a *genetic algorithm*, where the best candidates[9] in the previous generation are used to "seed" the next generation's offsets, while restricting the range for the variables of interest after each generation. The code was ran for three generations. The most promising candidates from the latest generation were used to obtain **THE** offsets to be used for subsequent analysis.

As an estimate of the systematic uncertainty associated with the use of these offsets, the yield in the $\pi^+$ missing mass peak was obtained for ∼200 sets of offsets for each 10.6 GeV **kaon_lt** kinematic setting. The standard deviation of these distributions is our estimate of this systematic effect. For all settings studied here this value was at, or below 0.05%.

[9]Set of offsets.

# References


[1] S. Ali *et al*, "The SHMS 11 GeV/c spectrometer in Hall C at Jefferson Lab", Nucl. Instrum. Meth. A 1083 (2026) 171070

[2] J. Volmer and H. Block, "Usage of Heepcheck", 1999, Hall C internal report.

[3] P. A. Adderley *et al*, "The Continuous Electron Beam Accelerator Facility at 12 GeV", Phys. Rev. Accel. Beams 27, 084802,
DOI: https://doi.org/10.1103/PhysRevAccelBeams.27.084802

[4] see: https://en.wikipedia.org/wiki/Voigt_profile or
https://reference.wolfram.com/language/ref/VoigtDistribution.html

[5] G. Niculescu, "JMU klt workflow", Hall C quarterly analysis meeting, 09/24/2025.

[6] " LMFIT: Non–Linear Least-Squares Minimization and Curve–Fitting for Python", see: https://lmfit.github.io/lmfit-py/#